Asian Journal of Chemistry; Vol. 24, No. 2 (2012), 589-594

ASIAN JOURNAL OF CHEMISTRY

www.asianjournalofchemistry.co.in

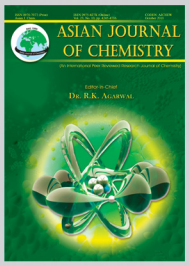

Study of Different Porous Size MCM-41 Molecular Sieve as Carrier of Captopril

JING-MEI LI[1], HUI YU[1], XIAO-DONG LI[1], QING-ZHOU ZHAI[1,*] and JIAN TIAN[2]

[1]Research Center for Nanotechnology, Changchun University of Science and Technology, Changchun 130022, P.R. China
[2]College of Life Science and Technology, Changchun University of Science and Technology, Changchun 130022, Jilin Province, P.R. China

*Corresponding author: Fax: +86 431 85383815; Tel: +86 431 85583118; E-mail: zhaiqingzhou@163.com; zhaiqingzhou@hotmail.com

(*Received*: 24 January 2011; *Accepted*: 10 October 2011) AJC-10487

In the study, two different porous size MCM-41 molecular sieves were synthesized by hydrothermal synthesis method under the different template and the prepared molecular sieves were used as the carrier of captopril drug. The structure of the prepared materials were characterized by powder X-ray diffraction, Fourier transform infrared spectra, nitrogen adsorption-desorption technique, transmission electron microscopy and scanning electron microscopy. The release process of the prepared drug was scouted in a simulated body fluid. During the drug release, it is found that the drug was rapidly released from the carrier during the first 1 h. After this, the release rate became comparative lentitude. For the (big-porous-MCM-41)-captopril sample (BC), the release rate was 50 % at 12 h and was 89 % at 36 h; for the (small-porous-MCM-41)-captopril sample (SC), it was 53 % at 5 h and was 99 % at 24 h.

Key Words: MCM-41 molecular sieve, Carrier, Captopril, Release.

INTRODUCTION

Control of drug release is a very important and very active area of research. The role of carriers in drug release process is mainly evaluated by the carried amount of drug and release rate of drug in delivery system[1]. Since the 21th century, considerable progress has been made in research on controlled drug release[2,3]. Many organic systems have been used as carriers of drug delivery systems, for example, capsules[4] and liposomes[5,6]. But these carriers have certain limitations, such as lower thermal stability and chemical stability, rapid decomposition in the immune system. In contrast, inorganic silica materials have extraordinary biological compatibility and stability and no additional harm to human body. Amorphous silica materials are non-toxic[7], often used as drug additives in the pharmaceutical field[8]. In addition, they can be transformed to $Si(OH)_4$ in the human body, then excreted from the body by excretory organs[9,10]. The research of silica gel and solid particles of silicon as the materials to control the process of drug release has been reported[11,12].

Mobil company has successfully synthesized MS41 series mesoporous molecular sieves in 1992[13]. This material has high surface area, large pore volume, narrow pore distribution and adjustable aperture, widely used in the fields of catalysis, adsorption separation, sensors, *etc*.[14-18]. As mesoporous materials have the unique superiority in the pore size distribution, some biological molecules such as the size of protein are in mesoporous range, thus mesoporous materials have their unique advantage and potential application in the separation of protein. The mesoporous structures of mesoporous materials have the characteristic of assembling organic macromolecules with biological activity, so they have got special application in the enzyme immobilization. The mesoporous materials also have important application foreground in biosensors and biochips. MCM-41 mesoporous molecular sieve has large specific surface area and specific pore volume, which can carry porphyrin and pyridine in the channels of materials or fix and embed protein and other biological drugs, to control drug release by modification of functional groups and improve the persistence of drug. Making use of biological guidance the medicine can effectively and accurately hit the targets such as cancer cells and lesions and develop its efficacy. For example, by impregnation method water-soluble anti-hypertension drug like D -3 - mercapto-2-methylpropionyl-L-proline is assembled in the channels of Si-MCM-41[19]. D-3-mercapto-2-methylpropionyl-L-proline/Si-MCM-41 sustained-release system can be obtained by measuring release rate of the assembly *in vitro* artificial gastric fluid. The direct embedding and controlled release of drugs are also good applications for mesoporous materials[20]. In recent years, greater attention have been paid on mesoporous materials as drug carriers with further research on the structures and properties of mesoporous molecular sieve[21,22]. Since mesoporous molecular sieves have uniform and adjustable pore channels and rich surface silanol can be

used as the new active sites in the reaction with organic guest molecules[23], to make drugs be binded to the active sites, uniformly dispersed into the channels of mesoporous molecular sieves, this can not only slow release of the absorbed drugs, but also adjust the effect through modification (such as ion-exchange to modify adsorption ability, surface modification to enhance interaction between its surface and drugs) to achieve better effect of controlled release[24].

The chemical name of captopril is (2S)-1-(3-mercapto-2-methylpropionyl) -L-proline, which is a kind of nonpeptide compounds, an orally active inhibitor of angiotensin-converting enzyme, used in the treatment of various hypertension. It can improve cardiac function of the patients with congestive heart failure and is effective especially for hypertension that is unresponsive to routine treatment[25]. In this study, different porous size MCM-41 molecular sieves were synthesized by hydrothermal synthesis method with cetyltrimethylammonium bromide and decyltrimethylammonium bromide as the template and the prepared MCM-41 molecular sieves were used as the carriers of captopril drug. The release process of the prepared drug was monitored in a simulated body fluid and the effect of different porous size MCM-41 carriers on captopril drug release rate was studied.

EXPERIMENTAL

Ethyl silicate (TEOS, A.R., Sinopharm Medicine Group, China); cetyltrimethylammonium bromide (CTMAB, A.R., Changzhou Xinhua Research Institute for Reagents, China); decyltrimethylammonium bromide (DTMAB, A.R., Nanjing Xuanguang Reagent Co. Ltd. China); octyltrimethylammonium bromide (OTMAB, A.R., Nanjing Xuanguang Reagent Co., Ltd. China); tetramethylammonium hydroxide (A.R., Shanghai Company of Chemical Reagents, Sinopharm Medicine Group, China); sodium hydrate (A.R., Kaiyuan Kangyuan Chemical Reagent Factory, China); captopril (Shanghai Pukang Pharmaceutical Co. Ltd., China.); the water for the experiment was deionized water.

The powder X-ray diffraction experiment was conducted with a D5005 X-ray diffraction analyzer (Siemens Company) and CuK_α was selected as the target material. The selected wavelength of X-ray was $\lambda = 1.5418$ Å; operating voltage (tube voltage) was 30 kV; operating current (tube current) was 20 mA. Fourier transform infrared spectroscopy was accomplished with BRUKER Vertex-70 FTIR Analyzer. KBr pellet technique (the proportion of the sample was 1 wt %, KBr was 99 wt %) was used to characterize vibration situation of material's backbone structure. The low-temperature nitrogen adsorption-desorption test was conducted on the Micromeritics ASAP2010M adsorption analyzer with test temperature of 77 K, to determine the pore structure of molecular sieves (pore size, pore volume, specific surface area, *etc*.). The samples were degassed under vacuum at 573 K for 12 h. Transmission electron micrograph (TEM) was recorded with the JEOL 2010 transmission electron microscope. Scanning electron micrograph (SEM) was measured with the JEOL JSM-5600 L scanning electron microscope. The catalytic spectrophotometric method was used for the determination of component content of captopril in the prepared nanodrug and captopril release process[25]. A 722S spectrophotometer (Shanghai Lingguang Technique Co. Ltd., China) was used for the tests to determine component content of captopril in the prepared host-guest nanocomposite and captopril release process in the simulated body fluid.

Process of the experiment

Synthesis of different porous size MCM-41 molecular sieves: Synthesis of big -porous-MCM-41: 1.0 g of CTMAB was added into 480 mL of deioned water at 80 ºC under vigorous stirring until the solution became homogeneous and 3.5 mL of 2 mol L^{-1} NaOH solution was added with stirring well, then 5 mL of TEOS was slowly added dropwise, reacted at 80 ºC for 2 h, then filtered, washed with deionized water and dried at room temperature to get the powder sample. The original sample was calcined in a muffle furnace at 500 ºC for 4 h and nano-MCM-41 sample was finally obtained[26].

Synthesis of small -porous-MCM-41 by the method from reference[27]: 1.04 g of DTMAB and 2.42 g of OTMAB were dissolved in 70.6 mL of water. 2.5 mL of TEOS was dissolved in 11.8 mL of tetramethyl ammonium hydroxide until the reaction was complete. The obtained solution was added to the previous template solution and then 22.5 mL of TEOS was dropped slowly into the solution. After the reaction was complete, the solution was transferred into a Teflon-lined autoclave, heated at 100 ºC for 24 h. Finally, the product was filtrated, washed, dried and calcined at 550 °C and then the template was removed to obtain white powdered target product.

Assembly of captopril in MCM-41: The liquid transplantation method was adopted in this study for the assembly of captopril drug into MCM-41 molecular sieves. Specific operation was as follows: (1) Big-porous-MCM-41 powder and small -porous-MCM-41 powder each 0.5 g were placed into 250 mL beakers, respectively. 100 mL of captopril ethanol solution was added in each beaker (at a concentration of 53 mg / mL), stirred for 48 h at room temperature (20 ºC). (2) The above mixed solutions were filtrated, washed, dried at room temperature. The samples prepared were put in a brown bottle, stored in a dryer, big-porous-MCM-41 as carrier labeled as BC, small -porous-MCM-41 as carrier labeled as SC.

Simulation experiment on captopril release process: A certain amount of the prepared drug powder was soaked in 50 mL simulated body fluid at 37 ºC[28] with magnetic force stirring. The content of captopril in the solution was measured by spectrophotometric method every 1-2 h[25]. In each process, great care was taken to add the same amount of simulated body fluid to supplement the solution when the mixed solution was removed to measure each time.

Distribution of simulated body fluid: NaCl (7.996 g), $NaHCO_3$ (0.350 g), KCl (0.224 g), $K_2HPO_4{\cdot}3H_2O$ (0.228 g), $MgCl_2{\cdot}6H_2O$ (0.305 g), 1 mol L^{-1} HCl (40 mL), $CaCl_2$ (0.278 g), Na_2SO_4 (0.071 g) and $NH_2C(CH_2OH)_3$ (6.057 g) were dissolved in distilled water and transferred in a 1000 mL volumetric flask and diluted up to the mark with distilled water[27].

RESULTS AND DISCUSSION

X-Ray diffraction analysis (XRD): Fig. 1 is the small-angle X-ray diffractogram of the prepared samples. In the

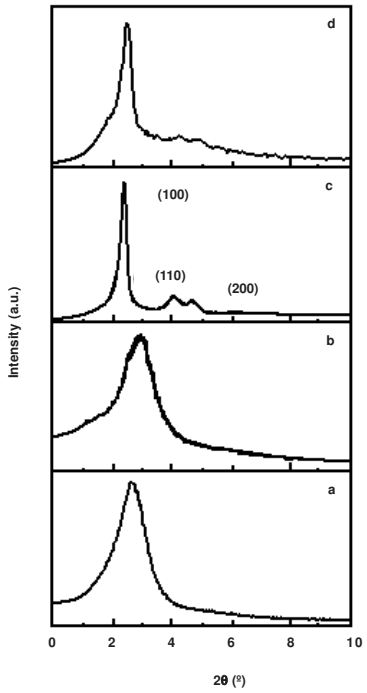

Fig. 1. Small-angle XRD patterns: a. Small -porous -MCM-41; b. SC; c. big-porous -MCM-41; d. BC

study, the prepared wide-angle MCM-41 sample (Fig. c) showed three distinct diffraction peaks at 2θ = 2.61°, 2θ = 4.1° and 2θ = 4.7°. The peaks were produced by (100), (110) and (200) crystal diffraction. BC sample (Fig. d) appeared only one distinct diffraction peak at 2θ = 2.5°, corresponding to big-porous MCM-41 powder. It indicated that the crystallinity of the material decreased after assembly of drug in MCM-41, but its 2D hexagonal pore structure was preserved. Small-porous MCM-41 sample (Fig. a) and SC sample (Fig. b) showed one diffraction peak at 2θ = 2.64° and 2θ = 3.02°, respectively. It showed that in the study the crystallinity of prepared small-porous MCM-41 and its sample carried with drug was found lower than that of big-porous MCM-41 sample, but its hexagonal pore structure was still preserved. Fig. 2 is the wide-angle X-ray diffractogram of the prepared samples. It can be seen from Fig. 2 that captopril powder showed a series of diffraction peaks in the measured range. But all the prepared samples did not show distinct diffraction peak at wide-angle. It indicated that in the assembling process captopril was mainly distributed in the pores of MCM-41 molecular sieve and captopril drug did not gather on the surface of molecular sieve.

Fourier transform infrared (FT-IR)spectra: Fig. 3 showed that all the prepared samples presented four characteristic absorption peaks in the measured range. The attribution of the peaks was shown in Table-1. Fig. (a) shows the infrared spectrum of captopril powder in the measured range. Compared with captopril powder the infrared spectra of SC sample (Fig. c) and BC sample (Fig. e) did not appear notable characteristic absorption peak of captopril drug. Their infrared absorption spectra were consistent with those of the corresponding MCM-41 powder. The existence of this phenomenon showed that on the one hand the skeleton of MCM-41 was well-preserved and the prepared drug was still pore structure after MCM-41

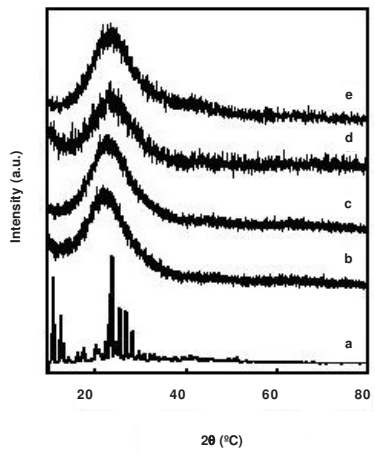

Fig. 2. Wide-angle XRD patterns: a. Captopril; b. Small -porous -MCM-41; c. SC; d. Big-porous -MCM-41; e. BC

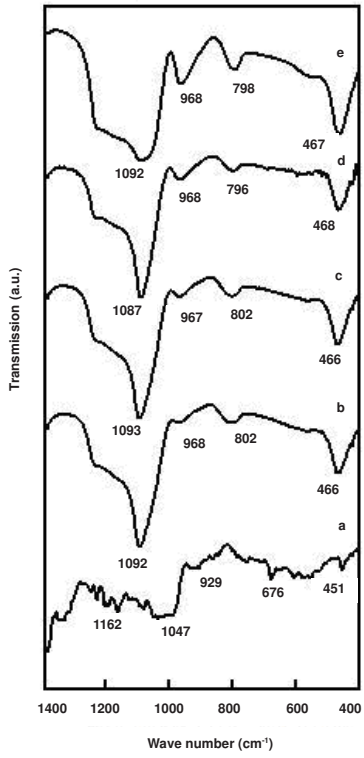

Fig. 3. Infrared spectra of each sample: (a) Captopril; (b) small-porous MCM-41; (c) SC, (d) big-porous MCM-41, (e) BC

TABLE -1
FOURIER TRANSFORM INFRARED ABSORPTION PEAKS

	Si-O-Si asymmetric stretching absorption peaks	Si-OH symmetric stretching absorption peaks	Si-O-Si symmetric stretching absorption peaks	Si-O-Si bending vibration absorption peaks
Big-porous MCM-41	1087	968	796	468
Small-porous MCM-41	1092	968	802	466
BC sample	1092	968	798	467
SC sample	1093	967	802	466

loaded with captopril. On the other hand, no characteristic absorption peak of captopril was found in the infrared spectra of the prepared drugs to show that the drug guest was mainly distributed in the channels of molecular sieves and there was no gathered guest material distributed on the outer surface of the carrier.

Analysis of nitrogen adsorption and desorption: Fig. 4 referred to the nitrogen adsorption and desorption isotherms of prepared materials. From this figure it is seen that nitrogen adsorption and desorption isotherms are of IV-shape and they both had a clear adsorption and desorption branching. In a lower relative and differential pressure scope, the adsorption and reconciliation adsorption branching of the sample's nitrogen adsorption and desorption isothermal lines were overlapped in the same place, but when the relative and differential pressure increased to a certain degree, the adsorption branching and reconciliation adsorption branching jumped suddenly and turned up a H_1-shape hysteresis loop. This is mainly because N_2 adsorption in molecular sieve pore channels was unilayer at the very beginning and this procedure was reversible, the adsorption branching and reconciliation adsorption branching didn't jump and there was no hysteresis loop. But when the relative and differential pressure increased to a certain degree, agglomeration phenomenon of capillary condesation would occur, then the adsorption branching and reconciliation adsorption branching jumped and hysteresis occurred accordingly. When the pore channels were filled with nitrogen, the gas was mainly adsorbed on the material's surface at that time and this procedure was reversible, so the adsorption branching and reconciliation adsorption branching were overlapped together and the curve became very gentle. When the relative and differential pressure became larger, for the adsorption branching and reconciliation adsorption branching the second break occurred. At the same time, there was also a hysteresis phenomenon. This is because the micropores formed between molecular sieves particles. When the relative and differential pressure reached a certain degree, there would be the second phenomenon of capillary condensation. Generally speaking, differential pressure of the phenomenon of capillary condensation was related to aperture size. The bigger of the aperture, the bigger of differential pressure of the pheno-menon of capillary condensation. Fig. 5 is the aperture distribution curve of the prepared materials and the figure showed that the aperture distribution of the prepared materials was very narrow.

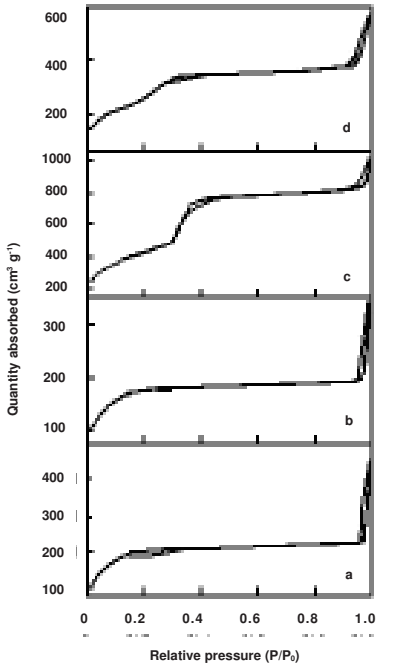

Fig. 4. Nitrogen adsorption-desorption isotherms: a) small -porous MCM-41; b) SC; c) big porous MCM-41; d) BC

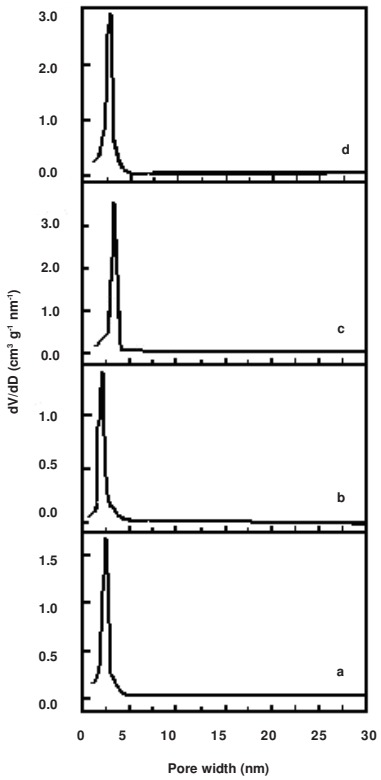

Fig. 5. Pore size distribution patterns of samples: a) small -porous MCM-41; b) SC; c) Big porous MCM-41; d) BC

Table-2 shows the pore structure parameters of the prepared materials, the specific surface area was calculated by BET (Brunner-Emmett-Teller)[29] and the distribution of aperture size was calculated by BJH (Barrett-Joyner-Halenda)[30]. The correlation data involved in each parameter's calculation were based on the adsorption branching of nitrogen adsorption and desorption isotherms. From the data it can be seen that compared the samples of SC and BC with the corresponding samples of small-porous (MCM-41) and big-porous (MCM-41), the specific surface area, pore volume and aperture were greatly reduced and this is mainly because the guest materials entered the subject pore channels. From this we can draw the conclusion that the guest materials of captopril have already entered into pore channels.

Transmission electron micrograph: Fig. 6 shows the transmission electron micrograph of each sample prepared in this study. Picture (a) was taken with the beam direction perpendicular to the pores and picture (b) was taken with the beam direction parallel to the pores. From the transmission electron micrograph it is seen that each sample was with the beam direction parallel to the pores had highly ordered pore structures

TABLE-2
PORE STRUCTURE PARAMETERS OF SAMPLES

Sample	BET surface area (m^2/g)	Pore volume[a] (cm^3/g)	Pore size[b] (nm)
Small–porous MCM-41	739.3	0.690	2.73
SC	621.1	0.599	2.46
Big-porous MCM-41	1329.1	1.331	3.55
BC	911.8	0.870	3.10

[a]BJH adsorption cumulative volume of pores. [b]Pore size calculated from the adsorption branch.

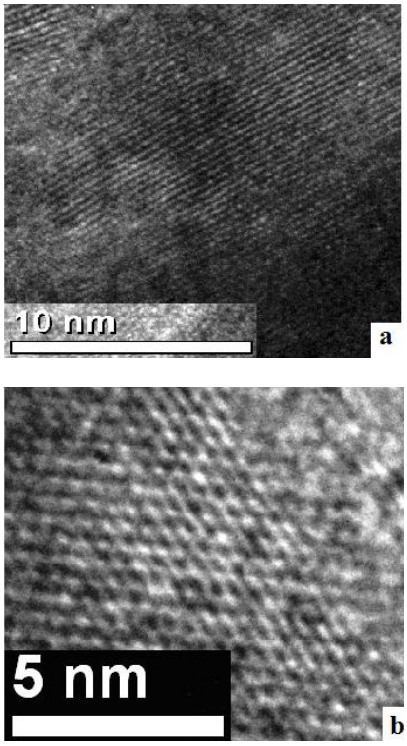

(A)

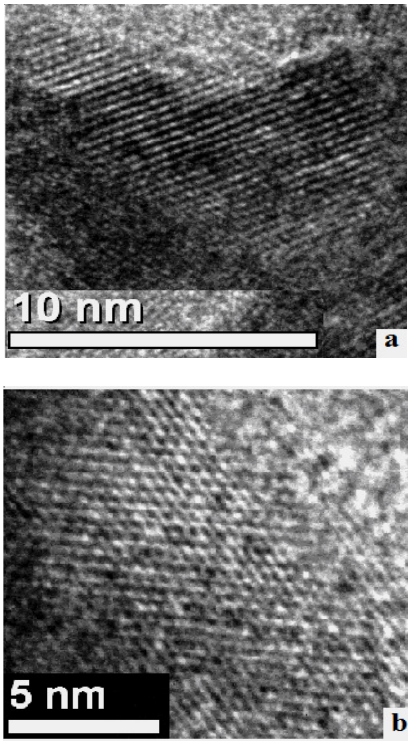

(B)

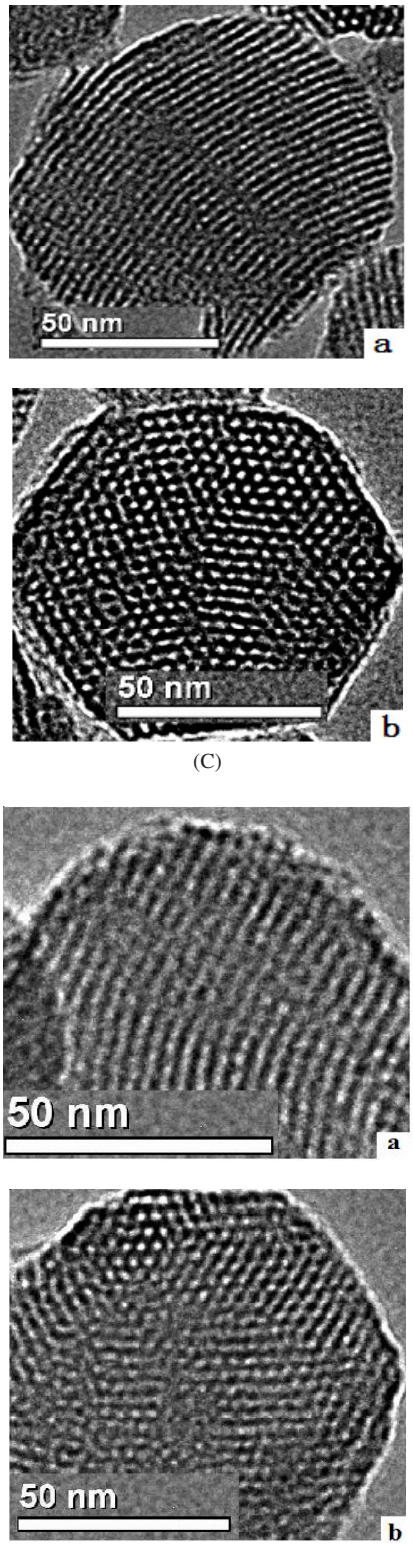

(C)

(D)

Fig. 6. TEM images of A) small porous MCM-41; (B) SC; (C) big porous MCM-41; (D) BC (a) taken with the beam direction perpendicular to the pores and (b) taken with the beam direction parallel to the pores

and the sample which was with the beam direction perpendicular to the pores showed regular lattice construction image. From these transmission electron micrographs itis seen intuitively that the samples made in this research had mesopore pore channel structure of two dimensional planar hexagon,

after assembling guest materials of the drug in molecular sieve pores. The mesopore pore channels of molecular sieve planar hexagon had been preserved.

Release curve of captopril: Fig. 7 shows the release curve of captopril in simulated body fluid. From the curve it is find that the drug was rapidly released from the carrier during the first 1 h. The release rate of sample BC was 25 % at 1 h, while the release rate of sample SC was 36 % at 1 h, due to the drug distributed on the surface and nearby the pores of MCM-41 was contacted with the body fluid directly and rapidly released. Not long after that, because the pore resistance was getting bigger and bigger when the body fluid entered into the pores of the carrier and the release rate became comparatively slow. For the sample BC, the release rate was 50 % at 12 h and was 89 % at 36 h; for the sample SC, it was 53 % at 5 h and was 99 % at 24 h. On comparing with the release process of sample BC and sample SC, it is found that the release rate of sample BC was much slower. This was because the pore diameter, specific surface area and pore volume of sample SC were much smaller than that of sample BC (Table-2), it is to explain the hole wall of sample SC was much thicker, but the pore channel was much smaller, so the guest drug distributed on the surface of carrier was much more than sample BC and its release rate was much faster than the drug in the pores. On the other hand, due to the small pore, the more prominent the siphon phenomenon became, the longer would the solution enter the pore. So it could promote the drug release and reduced the function of carrier for controlled-release.

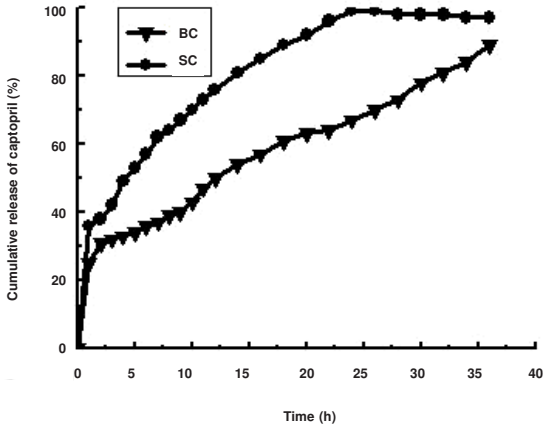

Fig. 7. Release curve of captopril

Conclusion

In this study, different porous size MCM-41 molecular sieves were synthesized, then captopril was assembled to molecular sieves pores by liquid-phase grafting method and served as the carriers of captopril drug. It was used to follow-up the release processes of prepared drugs in the simulated body fluid. Through the simulated release process, it was found that the drug was rapidly released from the carrier during the first 1 h. The release rate of sample (BC) was 25 % at 1 h and the release rate of sample (SC) was 36 % at 1 h. After this, the release rate became comparatively slow. For the sample (BC), the release rate was 50 % at 12 h and was 89 % at 36 h. For the sample (SC), it was 53 % at 5 h and was 99 % at 24 h. Compared with the release processes of sample (BC) and sample (SC), the release rate of sample (BC) was much slower and it had a better slow release. MCM-41 molecular sieves can be served as the carriers of captopril drug, which can greatly reduce the release rate of drugs, plays a role in slow release and improves drug's efficacy and efficiency.

ACKNOWLEDGEMENTS

The authors are grateful to the financial support from Department of Education of Jilin Province, P.R. China (Grant No. 2010JYT10,KYC-JC-XM-2010-014).

REFERENCES

1. Y.F. Zhu, J.L. Shi, W.H. Shen, H.R. Chen, X.P. Dong and M.L. Ruan, *Nanotechnology*, **16**, 2633 (2005).
2. M.J. Rathbone, J. Hadgraft and M.S. Roberts, Dekker, New York, p. 56 (2003).
3. A. Gopin, N. Pessah, M. Shamis, C. Rader and D. Shabat, *Angew. Chem. Int. Edn Engl*., **42**, 327 (2003).
4. K. Kataoka, A. Hrada and Y. Nagasaki, *Adv. Drug Delivery Rev*., **47**, 113 (2001).
5. D.L. Emerson, *Pharm. Sci. Technol. Today*, **3**, 205 (2000).
6. C. Oussoren and G. Storm, *Adv. Drug Delivery Rev*., **50**, 143 (2001).
7. C.T. Kresge, M.E. Leonowicz, W.J. Roth, J.C. Vartuli and J.S. Beck, *Nature*, **359**, 710 (1992).
8. M.F. Ottaviani, L. Mollo and B.J. Fubini, *Colloid Interf. Sci*., **191**, 154 (1997).
9. Z. Wu, J. Joo, H. Ahn, I.S. Kim, J.H. Kim and C.K. Lee, *J. Non-Cryst. Solids*, **342**, 46 (2004).
10. P. Kortesuo, M. Ahola, S. Laakso, I. Kangasniemi, A.Y. Urpo and J. Kiesvaara, *Biomater*., **21**, 193 (2000).
11. P. Kortesuo, M. Ahola, S. Karlsson, I. Kangasniemi, J. Kiesvaara and A.Y. Urpo, *J. Biomed. Mater. Res*., **44**, 162 (1999).
12. C. Barbe, J. Bartlett, L. Kong, K. Finnie, H.Q. Lin, M. Larkin, S. Calleja and A. Bush, *Adv. Mater*., **16**, 1959 (2004).
13. J.S. Beck, J.C. Vartuli, W.J. Roth, M.E. Leonowicz, C.T. Kresge, K.D. Schmitt, C.T.W. Chu, D.H. Olson, E.W. Sheppard, S.B. Mccullen, J.B. Higgins and J.L. Schlenkerr, *J. Am. Chem. Soc*., **114**, 10834 (1992).
14. N.Y. Yu, Y.J. Gong, S.G. Wang, D. Wu, Y.H. Sun, Q. Luo, W.Y. Liu and F. Deng, *Acta Chim. Sinica*., **61**, 58 (2003).
15. J.W. Zhao, F. Gao, Y.L. Fu, W. Jin, P.Y. Yang and D.Y. Zhao, *Chem. Commun*., 752 (2002).
16. X. Yuan, Y.Y. Liu, S.P. Zhuo, W. Xing, Y.Q. Sun, X.D. Dai, X.M. Liu and Z.F. Yan, *Acta Chim. Sinica*, **65**, 1814 (2007).
17. J.H. Zhu, W. Shen, H.L. Xu, Y.M. Zhou, C.Z. Yu and D.Y. Zhao, *Acta Chim. Sinica*, **61**, 202 (2003).
18. W.J. Xu, Q. Gao, Y.P. Xu, D. Wu and Y.H. Sun, *Acta Chim. Sinica*, **66**, 1658 (2008).
19. F.Y. Qu, G.S. Zhu, S.Y. Huang, S.G. Li and S.L. Qiu, *Chem. J. Chin. Univer*., **25**, 2195 (2004).
20. H.X. Guo, Y.M. Wang, H. Tang and Z.H. Cao, *Yunnan Chem. Indus*., **33**, 62 (2006).
21. C.Y. Lai, B.G. Trewyn, D.M. Jeftinija, K. Jeftinija, S. Xu, S. Jeftinija and V.S.Y. Lin, *J. Am. Chem. Soc*., **125**, 4451 (2003).
22. B. Munoz, A. Ramila, J. Perez-Pariente, I. Diaz and M. Vallet-Regf, *Chem. Mater*., **15**, 500 (2003).
23. A. Ramila, B. Munoz, J. Perez-Pariente and M. Vallet-Regí, *J. Sol-Gel Sci. Technol*., **26**, 1199 (2003).
24. L. Gao and J.H. Sun, *Acta Petrolei Sinica (Petroleum Processing Section)*, **24**, 265 (2006).
25. Z.H. Xie, K.S. Xue, H.Y. Lang and D.H. Lu, *Chin. J. Anal. Chem*., **31**, 1531 (2003).
26. Q. Cai, Z.S. Luo, W.Q. Pang, Y.W. Fan, X.H. Chen and F.Z. Cui, *Chem. Mater*., **13**, 258 (2001).
27. P. Horcajada, A. Ramila, J. Perez-Pariente and M. Vallet-Reg, *Micropor. Mesopor. Mater*., **68**, 105 (2004).
28. T. Kokubo, H. Kushitani and S. Sakka, *J. Biomed. Mater. Res*., **24**, 721 (1990).
29. S. Brunauer, P.-H. Emmett and E. Teller, *J. Am. Chem. Soc*., **60**, 309 (1938).
30. E.P. Barrett, L.G. Joyner and P.P. Halenda, *J. Am. Chem. Soc*., **73**, 373 (1951).